

Cite this: *RSC Adv.*, 2017, 7, 31129Received 28th April 2017  
Accepted 7th June 2017

DOI: 10.1039/c7ra04796g

rsc.li/rsc-advances

# Facile approach of Ni/C composites from Ni/cellulose composites as broadband microwave absorbing materials†

 Yun Wei,<sup>abc</sup> Xinxin Wang,<sup>ab</sup> Jingwei Zhang,<sup>b</sup> Haojie Liu,<sup>ab</sup> Xiaoyan Lv,<sup>b</sup>  
Miaomiao Zhang,<sup>b</sup> Shengchao Liu<sup>abc</sup> and Chunhong Gong<sup>id\*abc</sup>

In the current work, we synthesized Ni/C composites from Ni/cellulose composites and analyzed how well the products absorbed microwaves. The Ni/C composite products showed a maximal reflection loss (RL) of −53.8 dB at 4.72 GHz with a sample thickness of 4.5 mm, and the RL values exceeded −10 dB covers almost the whole tested frequency ranges (2–18 GHz). These results were attributed to a combination of the magnetic loss and the dielectric loss. This work is expected to contribute to the development of materials that absorb a broad region of the electromagnetic wave and to the recycling of cellulose.

## 1. Introduction

With the miniaturization of electronic components of integrated circuits, electromagnetic interference is becoming increasingly serious. At the same time, with the rapid development of microelectronic devices, the work frequency of the electronic components has gradually extended to the microwave region. The use of broadband microwave absorption materials (MAMs) is one of the most effective methods to solve the current electromagnetic radiation problem. According to principles of electromagnetism, the overall performance of a microwave absorber is mainly dependent on the complex permeability ( $\mu_r = \mu'_r + i\mu''_r$ ) and permittivity ( $\epsilon_r = \epsilon'_r + i\epsilon''_r$ ) of the components and the microstructures of the absorber.<sup>1–3</sup> The real and imaginary parts represent the storage and loss of electromagnetic wave energy in the absorbers, respectively. Generally, either only the magnetic loss or only the dielectric loss may induce a weak electromagnetic wave absorption due to the limited electromagnetic wave dissipation capability and the limited effective frequency band range. In this context, magnetic nanoparticles isolated from heterogeneous phases have been proven to be effective. For example, carbon-coated FeSn<sub>2</sub>/Sn,<sup>4</sup> Ni/oxide,<sup>5</sup> Ni<sub>3</sub>N/SiO<sub>2</sub>,<sup>6</sup> FeCo/polypyrrole (PPy),<sup>7</sup> and SiC-Fe<sub>3</sub>O<sub>4</sub><sup>8</sup> have been developed as high-efficiency broadband absorbers.

Cellulose fibers constitute an inexpensive and readily available natural material on earth, and their applications are broad due to their excellent biodegradability and renewability. In recent years, the utilization of cellulose fibers has become a hot topic in material research.<sup>9</sup> We previously fabricated Ni/cellulose composites with tunable magnetic and electrical properties by a facile *in situ* synthetic route.<sup>10</sup> We found that although the Ni nanoparticles were uniformly dispersed in and immobilized by the cellulose matrix, the prepared Ni/cellulose composites did not exhibit a strong response in the microwave region due to the cellulose not being an absorber of microwave radiation. In the current work, Ni/C composites were prepared by carrying out a direct carbonation reaction using the nickel/cellulose composites as reactants. Here, the cellulose turned into carbon, an exciting MAM, and the obtained Ni/C composites exhibited enhanced electromagnetic properties. Moreover, the obtained composites would produce significant synergetic effects resulting from heterogeneous electromagnetic couplings, such as interfacial polarizations and complementarity between the relative permittivity and permeability, allowing the prepared Ni/C composites to be used as a high-performance and broadband microwave-absorbing material.

## 2. Experimental

All the reagents were of analytical grade (Tianjin Kermel Chemical Company Ltd., Tianjin, China) and were used as received. First, Ni/cellulose composites were fabricated by following a facile *in situ* synthetic route based on our previous work.<sup>10</sup> Then, the obtained Ni/cellulose composites were subjected to carbonization by being heated at 800 °C for 4 h in a flowing H<sub>2</sub>/Ar (5 : 95) mixture gas to produce Ni/C composites.

The morphologies of the as-prepared samples were examined with a scanning electron microscope (SEM, JEOL JSM-5600LV)

<sup>a</sup>College of Chemistry and Chemical Engineering, Henan University, Kaifeng 475004, Henan, China. E-mail: gong@henu.edu.cn; Tel: +86-037123881589

<sup>b</sup>Engineering Research Center for Nanomaterials, Henan University, Kaifeng 475004, Henan, China

<sup>c</sup>Henan Engineering Research Center of Industrial Circulating Water Treatment, Henan University, Kaifeng 475004, Henan, China

† Electronic supplementary information (ESI) available. See DOI: 10.1039/c7ra04796g



and JEOL JEM-2010 transmission electron microscope (TEM, accelerating voltage 200 kV). A Philips X'Pert Pro X-ray diffractometer (XRD, Cu-K $\alpha$  radiation,  $\lambda = 1.5406 \text{ \AA}$ ) was used to analyze their phase compositions and microstructures. Raman scattering spectra were acquired using a confocal microscopic Raman spectrometer (RM-1000, Renishaw, England) with a 632.8 nm-wavelength laser as the excitation source. To test the electromagnetic properties of the obtained Ni/C composites, they were mixed with paraffin wax at a mass ratio of 45 : 55 and then pressed into cylindrically shaped compacts (inner diameter 3.04 mm, outer diameter 7.00 mm). The complex permeability and permittivity of the cylindrical compacts were recorded in the frequency range of 2.0–18.0 GHz with an Agilent N5230A network analyzer.

### 3. Results and discussion

Fig. 1(a) shows the XRD pattern of the obtained Ni/C composites. Diffraction peaks were observed at  $2\theta = 44.8^\circ$ ,  $52.2^\circ$  and  $76.6^\circ$ , which matched well with, respectively, the (111), (200), (220) crystal planes of the face-centered cubic lattice of nickel.<sup>11</sup> Moreover, a weak peak appeared at  $26.5^\circ$ , and corresponded to the (002) plane of graphitic carbon. The weak intensity of this peak indicated the relatively low degree of graphitization.<sup>12</sup> This result was further verified by acquiring a Raman spectrum of the obtained Ni/C composites as shown in Fig. 1(b). The composites exhibited both a peak at about  $1329 \text{ cm}^{-1}$ , attributed to disordered carbon and denoted as the D peak, and at about  $1604 \text{ cm}^{-1}$ , attributed to graphitic carbon and denoted as the G peak. Generally, the ratio of the intensity of the D peak to that of the G peak ( $I_D/I_G$ ) is calculated to determine the level of disorder in carbon-based materials. The value of  $I_D/I_G$  in the current work was calculated, using the software Origin 9.3/Peak Fitting Module, to be 1.9. This value indicated a considerable number of disordered and defect carbons.

The main panels of Fig. 2 show typical SEM images of the Ni/C composites. Moreover, a typical TEM image of the Ni/C composites is shown in the inset of Fig. 2(d). The samples for the TEM analysis were subjected to grinding and were dispersed into alcohol in the presence of ultrasonic stirring; a few drops of the resulting solution were introduced onto a carbon-coated copper grid and allowed to evaporate in air at room temperature. It could be found that the Ni particles with diameters

between 20 and 150 nm were evenly dispersed in the carbon matrix without aggregating, which is favorable for interacting with electromagnetic waves and could provide more opportunities for interfacial polarization under the action of an electric field or magnetic field. Thus, multiple reflections of electromagnetic waves and desired electromagnetic absorption properties were expected.

The magnetic loss factor ( $\tan \delta_M = \mu''/\mu'$ ) and dielectric loss factor ( $\tan \delta_E = \epsilon''/\epsilon'$ ) are the two main contributors to microwave absorption, and were calculated based on the measured permeability and permittivity values (as shown in Fig. S1†). Fig. 3(a) shows the magnetic loss factor and dielectric loss factor values of the sample. The value of  $\tan \delta_E$  was observed to decrease from 0.17 to 0.13 as the frequency was increased from 2.0 to 6.3 GHz, and then to increase as the frequency was increased further. The value of  $\tan \delta_M$  was observed to gradually increase as the frequency was increased from 2.0 to 5.5 GHz and then to decrease as the frequency was increased further. Evidently, the changes of  $\tan \delta_E$  and the  $\tan \delta_M$  with frequency were complementary.

Based on the transmit-line theory, the reflection loss (RL) of an absorbing material could be calculated from the relative complex permeability and permittivity. Fig. 3(b) shows the frequency-dependence of the RL values of the Ni/C-paraffin composites of different thicknesses. The absorption peaks were observed to shift toward the low-frequency regions as the absorber thickness was increased, and RL values of less than  $-10 \text{ dB}$  were found in the whole measured band (2–18 GHz) by adjusting the thickness of the absorbers from 1.0 to 10 mm. The lowest RL observed was  $-53.8 \text{ dB}$  at 4.72 GHz for a thickness of 4.5 mm, while RL under  $-20 \text{ dB}$  was achieved in very broad frequency range (2–10 GHz and 14–18 GHz) (as shown in Fig. S2†). Note that an RL value of  $-20 \text{ dB}$  corresponds to a 99% EM wave attenuation and materials with such an RL can be considered as effective absorbents in practical applications. Thus, our results indicated the prepared Ni/C composites to have excellent microwave absorption properties. The microwave absorbance of the paraffin composite was a result of the combination of the magnetic loss at 2.0–10.0 GHz and the dielectric loss at 14.0–18.0 GHz, and such values are indicative of a broadband EM wave absorber.

In the GHz frequency range, natural resonance and eddy current effects are commonly the main contributors to magnetic loss. The eddy current loss is related to the depth of the particle ( $d$ )

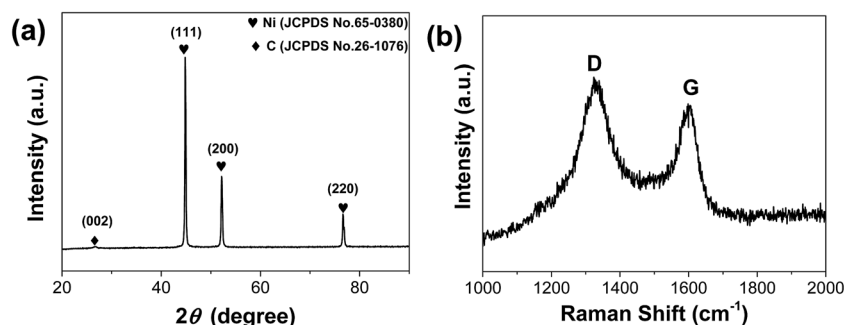


Fig. 1 XRD pattern (a) and Raman spectra (b) of the as-synthesized Ni/C composites.



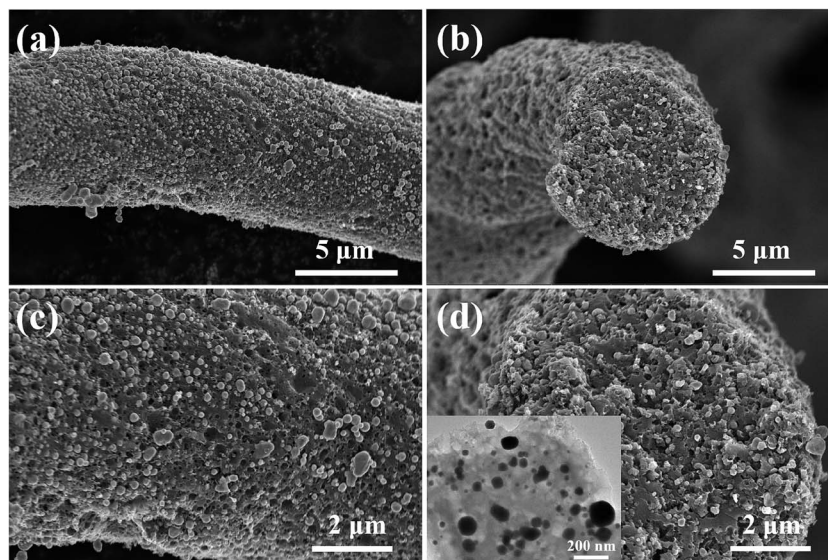


Fig. 2 SEM images of the surface ((a) and (c)) and cross-section ((b) and (d)) of as-synthesized Ni/C composites. The inset in (d) shows a TEM image of the corresponding Ni/C composites after having been subjected to grinding.

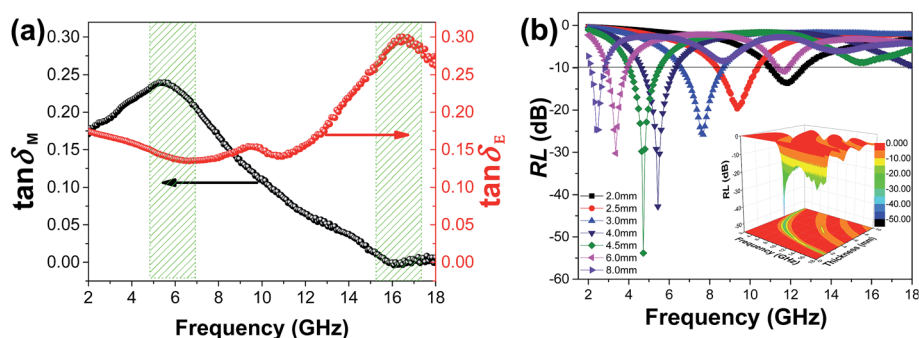


Fig. 3 Magnetic and dielectric loss factor (a) and of the calculated RL (dB) (b) of the Ni/C-paraffin composites as functions of frequency (a, b) and absorber thickness (b). The inset in (b) shows the corresponding three-dimensional representation of RL values for the composites at different thicknesses.

and the electric conductivity ( $\sigma$ ), which can be related to each other by the equation  $\mu''_r \approx 2\pi\mu_0(\mu'_r)^2\sigma d^2 f/3$ , where  $\mu_0$  is the vacuum permeability. According to this equation, if the magnetic loss only comes from the eddy current loss,  $C_0 \approx \mu''_r(\mu'_r)^{-2}f^{-1}$  should be constant and the  $C_0$  value depends on the particle diameter and the electric conductivity at the varying frequency.<sup>13</sup>

As shown in Fig. 4(a), the  $C_0$  value of the sample was nearly the same at every frequency tested. Thus, it is reasonable to conclude that the eddy current loss was the main contributor to the magnetic loss. This relationship between eddy current loss and magnetic loss was consistent with the rapid decrease of  $\mu'_r$  at high

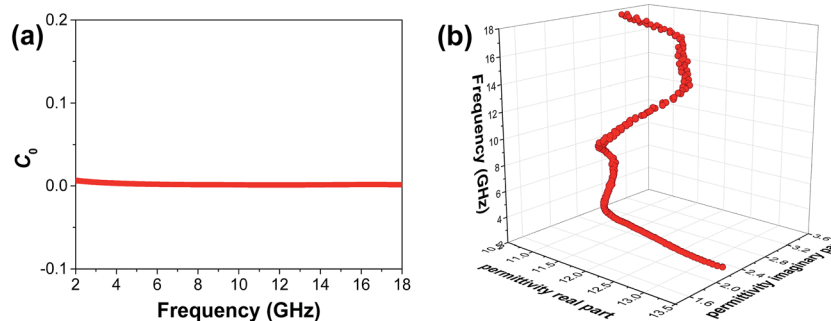


Fig. 4 The values of  $C_0$  ( $C_0 = \mu''_r(\mu'_r)^{-2}f^{-1}$ ) of the Ni/C-paraffin composites (a) and the Cole-Cole semicircles of the complex permittivity (b).



frequencies and the imaginary part  $\mu''_r$  having reached a maximum at a lower frequency (as shown in Fig. S1†).

In the Debye theory,  $\epsilon''_r$  stands for the electromagnetic wave dissipation capability in absorbers. The relationship between  $\epsilon'_r$  and  $\epsilon''_r$  could be plotted according to the eqn (1) and each Cole–Cole semicircle corresponds to one Debye relaxation process.<sup>14</sup>

$$\left(\epsilon' - \frac{\epsilon_s + \epsilon_\infty}{2}\right)^2 + \epsilon''^2 = \left(\frac{\epsilon_s - \epsilon_\infty}{2}\right)^2 \quad (1)$$

To investigate the dielectric polarizations of the Ni/C composites, the Cole–Cole plots of the complex permittivity were made, and are shown in Fig. 4(b). The large semicircle suggested that dipolar polarization relaxation processes occurred, which we believed resulted in the strong dielectric loss for the sample. The elevated level of interfacial polarization relaxation was ascribed to the high heterogeneous interface between the Ni nanoparticles and the carbon matrix. Under an electromagnetic field, these dielectric relaxations can transform electromagnetic energy to heat energy, causing the profound loss of microwave absorbance.

## 4. Conclusions

In summary, the Ni/C composites were synthesized by calcining Ni/cellulose composites, and the microwave absorbance of the product was analyzed. Due to the combination of the magnetic loss and the dielectric loss, the obtained Ni/C composites showed promising potential as a high-performance and broadband microwave-absorbing material. Notably, the RL values exceeded −10 dB throughout nearly the entire spectrum (2–18 GHz). This work has provided a new potential contribution to both the development of materials that absorb a broad region of the electromagnetic spectrum and to the recycling of cellulose.

## Acknowledgements

This work was financially supported by the National Natural Science Foundation of China (grant No. 21671057, 21271063, and

51471045), the Program for Innovative Research Team from the University of Henan Province (16IRTSTHN015), and the Foundation for Youth Key Teachers of Henan Province (GGJS-024).

## References

- 1 G. L. Wu, Y. H. Cheng, Q. Xie, Z. R. Jia, F. Xiang and H. J. Wu, *Mater. Lett.*, 2015, **144**, 157.
- 2 H. J. Wu, G. L. Wu, Y. Y. Ren, L. Yang, L. D. Wang and X. H. Li, *J. Mater. Chem. C*, 2015, **3**, 7677.
- 3 Y. P. Duan, J. Liu, Y. H. Zhang and T. M. Wang, *RSC Adv.*, 2016, **6**, 73915.
- 4 X. F. Zhang, Y. Rao, J. J. Guo and J. W. Qin, *Carbon*, 2016, **96**, 972.
- 5 B. Zhao, G. Shao, B. B. Fan, W. Li, X. X. Pian and R. Zhang, *Mater. Lett.*, 2014, **121**, 118.
- 6 Y. S. Jia, H. S. Pan, H. J. Meng, H. J. Liu, Z. Q. Wang, X. Li, L. L. Zhu, P. Chai and C. H. Gong, *RSC Adv.*, 2015, **5**, 14061.
- 7 H. C. Wang, Z. R. Yan, J. An, J. He, Y. L. Hou, H. Y. Yu, N. Ma, G. H. Yu and D. B. Sun, *RSC Adv.*, 2016, **6**, 92152.
- 8 C. Y. Liang, C. Y. Liu, H. Wang, L. N. Wu, Z. H. Jiang, Y. J. Xu, B. Z. Shen and Z. J. Wang, *J. Mater. Chem. A*, 2014, **2**, 16397.
- 9 L. Chen, T. Ji, L. W. Mu and J. H. Zhu, *Carbon*, 2017, **111**, 839.
- 10 C. H. Gong, X. X. Wang, H. J. Liu, C. Zhao, Y. D. Zhang, Y. S. Jia, H. J. Meng, J. W. Zhang and Z. J. Zhang, *Cellulose*, 2014, **21**, 4359.
- 11 S. Qiu, H. L. Lyu, J. R. Liu, Y. Z. Liu, N. N. Wu and W. Liu, *ACS Appl. Mater. Interfaces*, 2016, **8**, 20258.
- 12 Y. C. Yin, X. F. Liu, X. J. Wei, R. H. Yu and J. L. Shui, *ACS Appl. Mater. Interfaces*, 2016, **8**, 34686.
- 13 X. A. Li, X. J. Han, Y. C. Du and P. Xu, *J. Magn. Magn. Mater.*, 2011, **323**, 14.
- 14 M. K. Han, X. W. Yin, L. Kong, M. Li, W. Y. Duan, L. T. Zhang and L. F. Cheng, *J. Mater. Chem. A*, 2014, **2**, 16403.

